Department of Pharmaceutics[1], China Pharmaceutical University, Nanjing; Jiangsu Province Academy of Traditional Chinese Medicine[2], Nanjing; Qilu Pharmacutical Co., Ltd.[3], Shandong, China

Preparation, physicochemical characteristics and bioavailability studies of an atorvastatin hydroxypropyl-β-cyclodextrin complex

Hui-Xia Lv[1], Zhen-Hai Zhang[2], Hui-Jiang[3], Ayman Y. Waddad[1], Jian-Ping Zhou[1]

Received June 17, 2011, accepted July 11, 2011

Dr. Zhen-Hai Zhang, Jiangsu Province Academy of Traditional Chinese Medicine, Nanjing, China.
Prof. Jian-Ping Zhou, Department of Pharmaceutics, China Pharmaceutical University, Nanjing, China
davidpharm@yeah.net (Zhen-Hai Zhang); iamzhoujianping@163.com (Jian-Ping Zhou)

Pharmazie 67: 46–53 (2012) *doi: 10.1691/ph.2012.1082*

The aim of this study was to improve the solubility, stability and bioavailability of amorphous atorvastatin calcium (AT) by complexing it with hydroxypropyl-β-cyclodextrin. The formation of the inclusion complexation was identified by molecular modeling, phase solubility diagrams, differential scanning calorimetry and X-ray powder diffractometry. Orally Disintegrating Tablets (ODT) were then manufactured by direct compression. Apart from improved stability compared to pure AT, disintegration time of 27 s, hardness of 5 kg and favorable mouth feel were achieved. *In vitro* dissolution tests of the ODT of AT inclusion complex exhibited higher dissolution rates than those with pure drug and the commercial tablet Lipitor®. *In vivo* bioavailability studies in rats also showed shorter T_{max}, higher C_{max} and increased AUC of 4.42 and 1.86 fold compared to the plain drug ODT and Lipitor®. These results strongly suggest to use HP-β-CD to improve the physicochemical characteristics and bioavailability of AT.

1. Introduction

Cyclodextrins are cyclic oligomers composed of several D-glucose units bonded by α-(1, 4) linkages. This provides a molecule shaped like a segment of a hollow cone able to form inclusion complexes with various molecules. Complexation with cyclodextrin has been reported to improve physicochemical properties like solubility, dissolution rate and stability of drugs consequently enhancing bioavailability (Loftsson and Brewster 1996; Frömming and Szejtli 1994). The chemical modification of amorphous hydroxypropyl-β-cyclodextrin (HP-β-CD) by partial etherification of the crystalline parent cyclodextrin with a hydroxyalkyl group, achieves higher water solubility, greater complexing properties, lower irritancy and toxicity than β-cyclodextrin (Yaksh et al. 1991; Gould and Scott 2005). Furthermore HP-β-CD has proved to be widely used in the field of drug encapsulation (Yang et al. 2008; Ben Zirar et al. 2008).

Atorvastatin calcium (AT) is a synthetic reversible inhibitor of 3-hydroxy-3-methylglutaryl-coenzyme A (HMG-CoA) reductase, which is indicated as an adjunct to diet for the prevention of cardiovascular disease and for treatment of patients with hypercholesterolemia, primary dysbetalipoproteinemia, or other forms of dyslipidemia. It is also used to reduce the risk of myocardial infarction, stroke, and heart failure in people with type 2 diabetes but without evidence of heart disease (Kappelle et al. 2010; Foody et al. 2008). AT is currently available as tablets under the brand name "Lipitor®" manufactured by Pfizer, a top-selling branded pharmaceutical (Simons 2003). However, the marketed formulation is marred with the problem of poor oral bioavailability (12%) (Kim et al. 2008) due to the drug's poor water-solubility and pre-systemic clearance in gastrointestinal mucosa and hepatic first-pass metabolism. AT has also been shown to be sensitive to the pH of the environment, humidity, light, temperature and oxygen (Khedr 2007).

In the present study, an inclusion complex of AT with HP-β-CD was prepared by ultrasound and rotary evaporating methods. The physicochemical properties of the formed inclusion complex were characterized by different analytical techniques, such as molecular modeling, phase solubility diagrams, differential scanning calorimetry and X-ray powder diffractometry etc. It was particularly formulated as orally disintegrating tablets (ODT) to partly resolve the problem of first-pass metabolism in gut and liver and hence enhance the bioavailability of the drug. Furthermore an ODT formulation of AT would improve the patient compliance especially for the elderly population, and offer an alternative for the only available conventional tablet dosage form.

2. Investigations and results

2.1. Molecular-modeling studies

The side and top views resulting from the molecular modeling of HP-β-CD after energy minimization (Figs. 1a and 1b) are correlated to the AT molecule (Fig. 1c).

The superior and inferior caliber of HP-β-CD were determined to be 8.7 Å and 7.7 Å respectively while the diameter of AT cephalic region was 7.9 Å, this indicated AT could be engulfed into the cavity of HP-β-CD but further investigations were need. The initial potential energy (Table 1) was noticed to have reduced after minimization of energy was performed, this was in line with the results obtained from the program in the simulation directory of DS 2.1 for calculating energy. The interaction energy as the sum of Van der Waals and electrostatic energy was –19.1713 and –136.12972 kcal/mol for HP-β-CD and AT, respectively. The least energy poses of AT in the complex with HP-β-CD resulting from the docking simulation using Dock Ligands (CDOCKER) could be illustrated as shown in Fig. 2.

Table 1: The Initial potential energy, potential energy, Van der Waals energy and electrostatic energy of AT and HP-β-CD

Name	Force field	Initial Potential Energy (Kcal/mol)	Potential Energy (Kcal/mol)	Van der Waals Energy (Kcal/mol)	Electrostatic Energy (Kcal/mol)
HP-β-CD	CHARMm	522.45054	99.10055	−19.44207	−131.87916
AT	CHARMm	126.29629	42.52221	0.27077	−4.25056

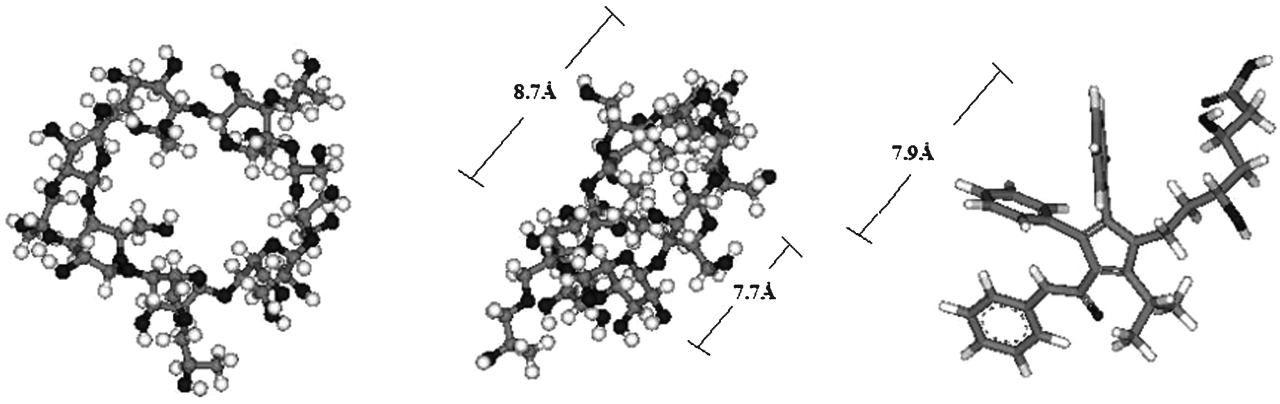

Fig. 1: HP-β-CD and AT views (a: HP-β-CD side view; b: HP-β-CD vertical view; c: AT view)

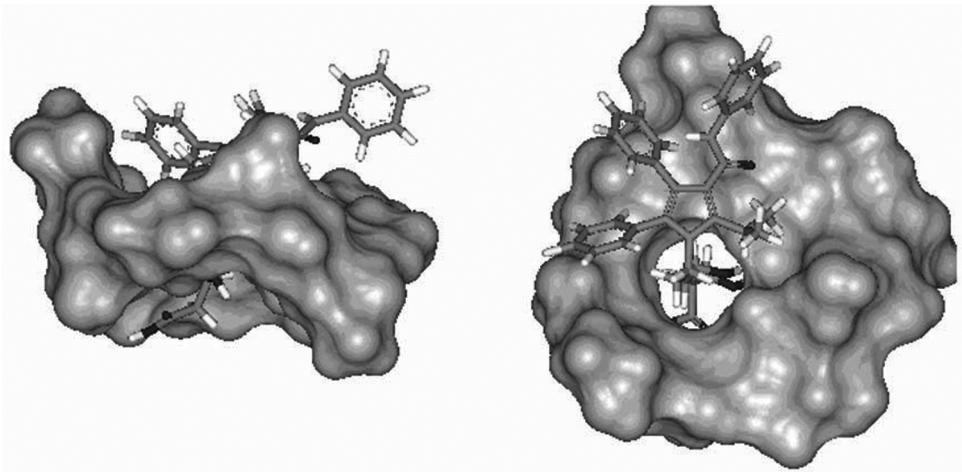

Fig. 2: Molecular docking diagrams of HP-β-CD and AT

By the side view and top view (Fig. 2) it was indicated that the AT molecule had been engulfed inside the cavity of HP-β-CD through the head region narrow rim (i.e. primary hydroxyl group). Binding energy was negative, suggesting that a spontaneously inclusion process.

Low binding and noticeable entropic energies imply a considerable sort of stability for the resultant complex, this was further confirmed by the presence of hydrogen and electrostatic bonds observed (Fig. 3).

2.2. Phase-solubility study

The phase-solubility diagram for complex formation between AT and HP-β-CD (Fig. 4) takes the type A_N pattern, this clearly indicated that complexation of AT with HP-β-CD increased AT solubility (Higuchi and Connors 1965). The shape of the A_N plot suggests that a different mechanism of inclusion was involved at low and at high concentrations of HP-β-CD (Fig. 4). The anterior part of the curve was linear; this indicated a 1:1 ratio in the low concentration of HP-β-CD solution for the inclusion complex present. While the nonlinear part of curve showed a decreased tendency which could be attributed to complicated inclusion between AT and HP-β-CD, such as formation of a super-molecule.

The complexation constant ($K_{1:1}$), as per hypothesis of 1:1 stoichiometric ratio of complexes, was calculated from the

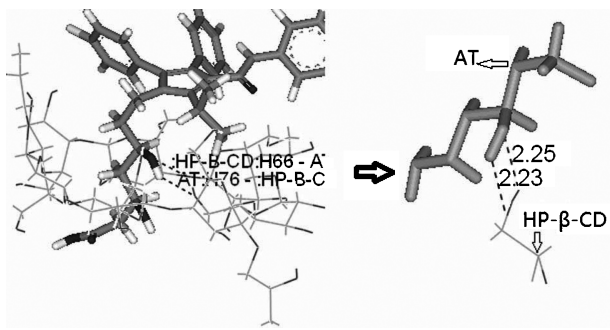

Fig. 3: Hydrogen and electrostatic bonds of AT with HP-β-CD

Table 2: Binding energy, complex energy and entropic energy of AT between with HP-β-CD

Ligand Name	Binding energy (kcal/mol)	Ligand energy (kcal/mol)	Protein energy (kcal/mol)	Complex energy (kcal/mol)	Entropic energy (kcal/mol)
AT	–24.29098	95.27553	616.390747	687.37530	22.32770

phase-solubility diagrams (Higuchi and Connors 1965) using the following Eq. (1).

$$K_{1:1} = \frac{Slop}{S_0(1 - Slop)} \quad (1)$$

where, $K_{1:1}$ was the complexation constant, S_0 was the intrinsic solubility, and the slope was calculated from a graph of the dissolved drug concentration verses HP-β-CD concentration in the medium. The intrinsic solubility value (S_0) of AT in the absence of HP-β-CD was determined directly in aqueous media. The Gibbs free energy (ΔG) values were calculated from the inclusion constants Eq. (2) and appropriately tabulated (Table 3). From ΔG values, other thermodynamic parameters including enthalpy (ΔH) and entropy (ΔS) could be obtained using the Van't Hoff equation (3). All parameters are shown in Table 3.

$$\Delta G = -RT \ln K_{1:1} \quad (2)$$

$$\frac{\Delta G}{T} = \Delta H \frac{1}{T} - \Delta S \quad (3)$$

where R was the gas constant, and T was the temperature in Kelvin; K1:1 was the complexation constant of AT with HP-β-CD.

$K_{1:1}$ and absolute ΔG value decreased with increasing temperature. This indicated that higher temperatures were unfavorable for the inclusion process. This could be explained by the increased movement of molecules at high temperatures, which leads to disassociation hence low temperatures were favorable for the inclusion process. All ΔG and ΔH values obtained for the inclusion processes (Tablet 3) were negative. This indicated that the inclusion proceeded exothermically and spontaneously.

2.3. Preparation of the inclusion complex

From preliminary studies the influencing factors such as the methods of preparation, the ratio of AT HP-β-CD and temperature were established. Based on those results, the molar ratio was kept at 1:6 (AT: HP-β-CD) and ultrasound method selected in all cases (Table 4). Furthermore from the procedure in item 4.2.3 the solubility of the inclusion complex (1:6) was determined to be 6.535 mg/ml which is realized to be 37 times that of pure AT (0.176 mg/ml).

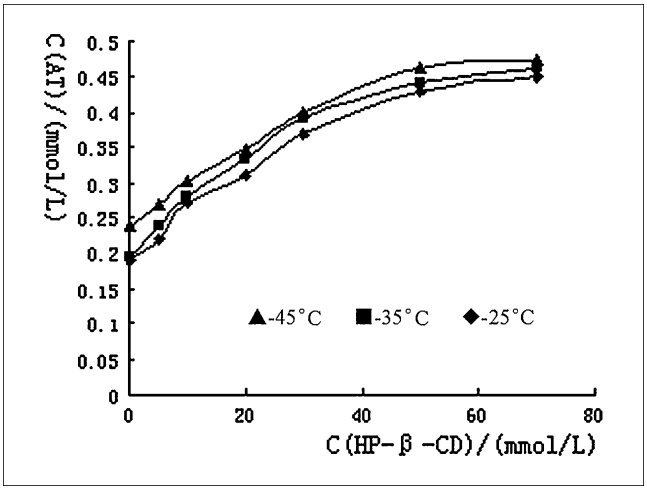

Fig. 4: Phase solubility curve of AT inclusion at 25 °C, 35 °C and 45 °C

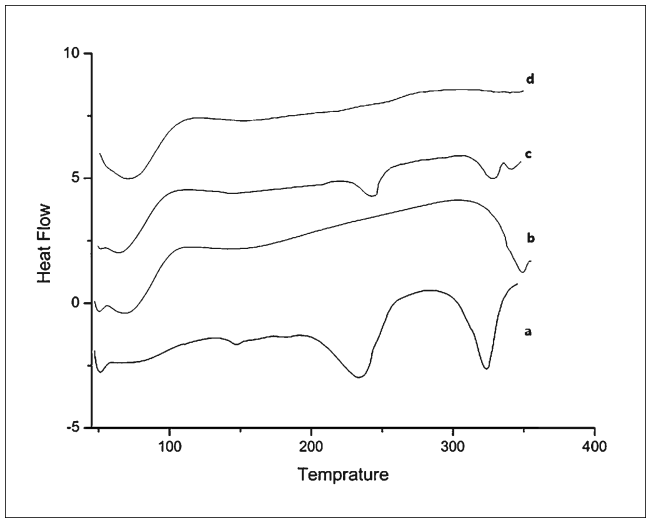

Fig. 5: DSC curves. a: AT, b: HP-β-CD, c: AT/HP-β-CD physical mixture, d: AT/HP-β-CD inclusion complex

Other factors such as humidity, temperature and exposure to light that could influence the stability of the inclusion complex were also investigated and compared to those of pure AT (experimental details not included due to space limit). After 10 days, there was no considerable difference in regard to degradation by humidity between the two (less 0.5%), however temperature changes gave rise to degradation by 10% for pure AT compared to 5% for inclusion complex. Exposure to light resulted in degradation by 7% for pure AT while 2.8% for inclusion complex. This indicated that inclusion complexing could be a promising method for stabilization.

2.4. Differential scanning calorimetry (DSC)

DSC thermograms were used to analyze the rate of heat absorbed by AT, HP-β-CD, AT/HP-β-CD physical mixture and AT/HP-β-CD (1:6) inclusion complex (Fig. 5). These analysis gave supporting evidence for the complexation of AT with HP-β-CD. The two characteristic endothermic DSC peaks around 240 °C and 325 °C (Fig. 5a) for AT are present in the thermograms of the physical mixtures but not in those of the inclusion complexes (Fig. 5d), which confirms the formation of the inclusion complexes.

2.5. Powder X-ray diffraction studies (PXRD)

The PXRD patterns for the crystal form of AT, amorphous AT, HP-β-CD, AT/HP-β-CD physical mixture and the corresponding inclusion complexes are presented in Fig. 6. The X-ray diffractograms of the amorphous AT, HP-β-CD and the corresponding inclusion complexes consisted fundamentally of a single broad band, comparing to that of the crystal form of AT, it indicated that the drug was not transformed to crystalline during the inclusion process.

Table 3: Thermodynamic parameters of inclusion in water

T(°C)	Linear equation	$K_{1:1}$ ($L \cdot mol^{-1}$)	ΔS ($J \cdot mol^{-1} \cdot K^{-1}$)	ΔH (KJ mol^{-1})	ΔG (KJ mol^{-1})
25	$y = 0.0122x + 2.0027$ $R^2 = 0.9038$	164.1557	–56.096	–29.335	–12.609
35	$y = 0.0185x + 1.9826$ $R^2 = 0.9612$	107.1676	–56.096	–29.335	–12.049
45	$y = 0.026x + 2.0298$ $R^2 = 0.9595$	78.06923	–56.096	–29.335	–11.488

Table 4: Entrapment efficiency and drug content of the three methods

Ratio	Grinding method (%)		Ultrasound method (%)		Stirring method (%)	
	Entrapment efficient	Drug content	Entrapment efficient	Drug content	Entrapment efficient	Drug content
1:2	41.7	13.9	40.8	13.6	39.6	13.2
1:3	53.2	13.2	55.1	13.8	51.8	13.0
1:4	58.1	11.6	49.7	10.01	57.1	11.4
1:5	64.6	10.7	73.8	12.3	62.8	10.5
1:6	70	10	104.3	14.9	69.5	9.9

2.6. Fourier transforms infrared spectroscopy (FT-IR)

Fourier Transform Infrared spectrophotometry (FTIR) is a useful tool for identifying drug excipient interactions (Crupi et al. 2007). In this study, FTIR spectroscopy provided important information for confirming formation of the inclusion complex. In the FTIR spectrum (Fig. 7) for pure AT, the absorption observed at 3408 cm^{-1} and between 1700–1400 cm^{-1} could be attributed to the stretching vibrations of the N–H and the C–C bond of aromatic ring. The peaks observed in this spectrum at 1400–1100 cm^{-1} reflects C–O, C–F groups' vibrations and 690–850 cm^{-1} reflects C-H bond bending vibrations of the benzene ring. It can be seen that the FTIR spectrum of the inclusion complex varies with that of the pure AT, for the three absorption bands (1700–1400 cm^{-1}, 1400–1100 cm^{-1} and 690–850 cm^{-1}). In addition, a slight red shift was observed for each of these bands in the spectrum obtained for the complexes.

The FTIR data revealed that part of benzene ring and a side chain of AT is specifically involved in the interaction between AT and HP-β-CD. The FTIR spectrum for the complexes showed a substantial decrease in intensity for the three bands associated with the AT groups. This result suggests the formation of a new supra-molecular compound. Additionally, no new peaks were observed in the spectra of AT complex systems, indicating no chemical bonds were created in the complex formation.

2.7. ^1H NMR study

NMR was effectively used to study space conformations of HP-β-CD inclusion, as it has been previously used to provide elaborate information about the stoichiometry, stability, and structure of CD complexes (Cabral Marques et al. 1990). The ^1H NMR diagrams of the pure AT, pure HP-β-CD and the complexes of the various AT: HP-β-CD ratios were showed in Fig. 8. In the spectrum of pure AT (Fig. 8a), the characteristic signals observed are for H1 (δ1.0–1.1 ppm), H2 (δ1.2–1.3 ppm), H3 (δ1.9–2.0 ppm), H4 (δ2.0–2.1 ppm), H5 (δ3.1–3.2 ppm),

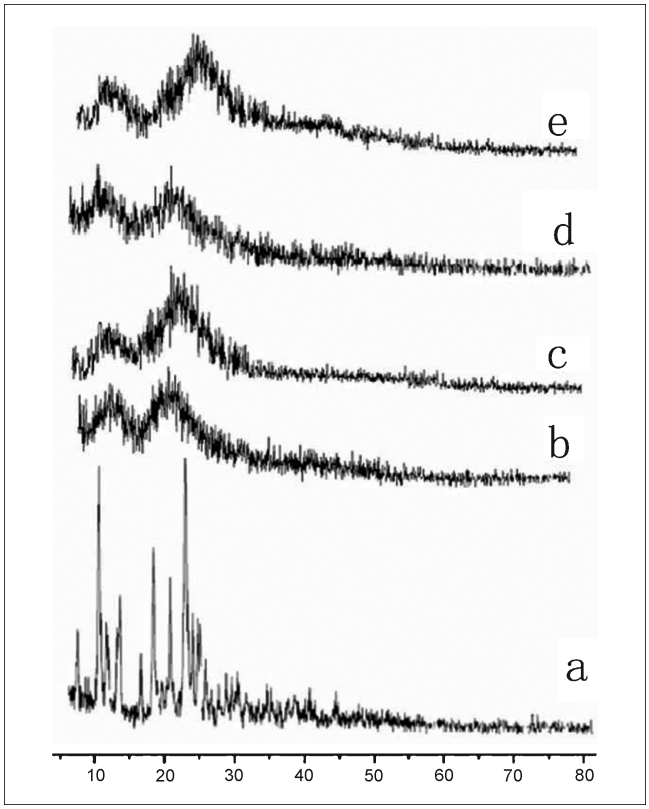

Fig. 6: X-Ray diagram; a: crystal form of AT, b: amorphous AT c: HP-β-CD, d: physical mixture of AT and HP-β-CD(1:6), e: inclusion complex of AT and HP-β-CD(1:6)

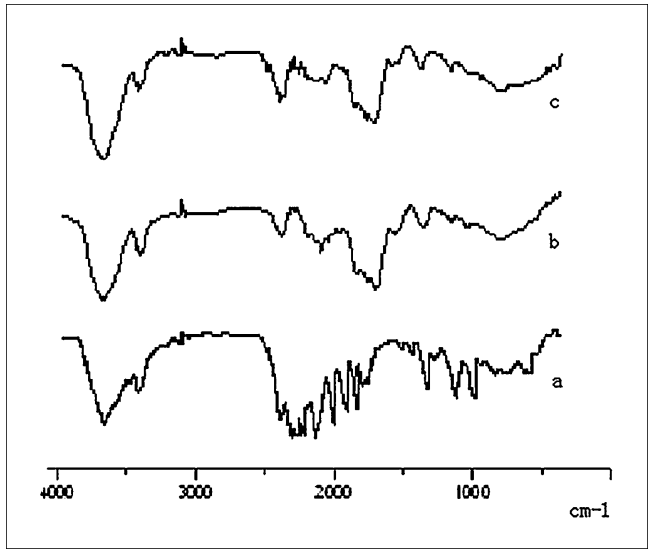

Fig. 7: FT IR spectra: a: AT, b: HP-β-CD, c: inclusion complex AT and HP-β-CD (1:6)

Table 5: ^{1}H NMR signal changes of AT

Samples	Characteristic signals								
Pure AT	H1	H2	H3	H4	H5	H6	H7	H8	H9
Complex (1:2)	↓	↓	–	–	–	–	=	↓	↓
Complex (1:6)	–	–	–	–	–	–	=	↓	↓

Note: (–) means loss, (=) means overlap, (↓)means low intensity

H6 (δ3.9–4.0 ppm), H7 (δ4.6–4.7 ppm), H8 (δ7.0 ppm) and H9 (δ7.2 ppm) (Fig. 9 and Table 5). The assignments and the chemical shift values of the various ratio of AT with HP-β-CD given in Fig. 8c and d was observed that the signal for H8 and H9 is persistent for inclusion complexes (1:2) and (1:6) but at low intensity. Meanwhile the signal for H1 and H2 existed at low intensity for the inclusion complex (1:2). The shifts of H7 of AT do overlap with those of HP-β-CD, but do not increase in intensity. Those results implied that the 1 and 4 parts (indicated on structure) of AT could be entered into the cavity of HP-β-CD and the suitable ratio for inclusion of AT into HP-β-CD is 1:6.

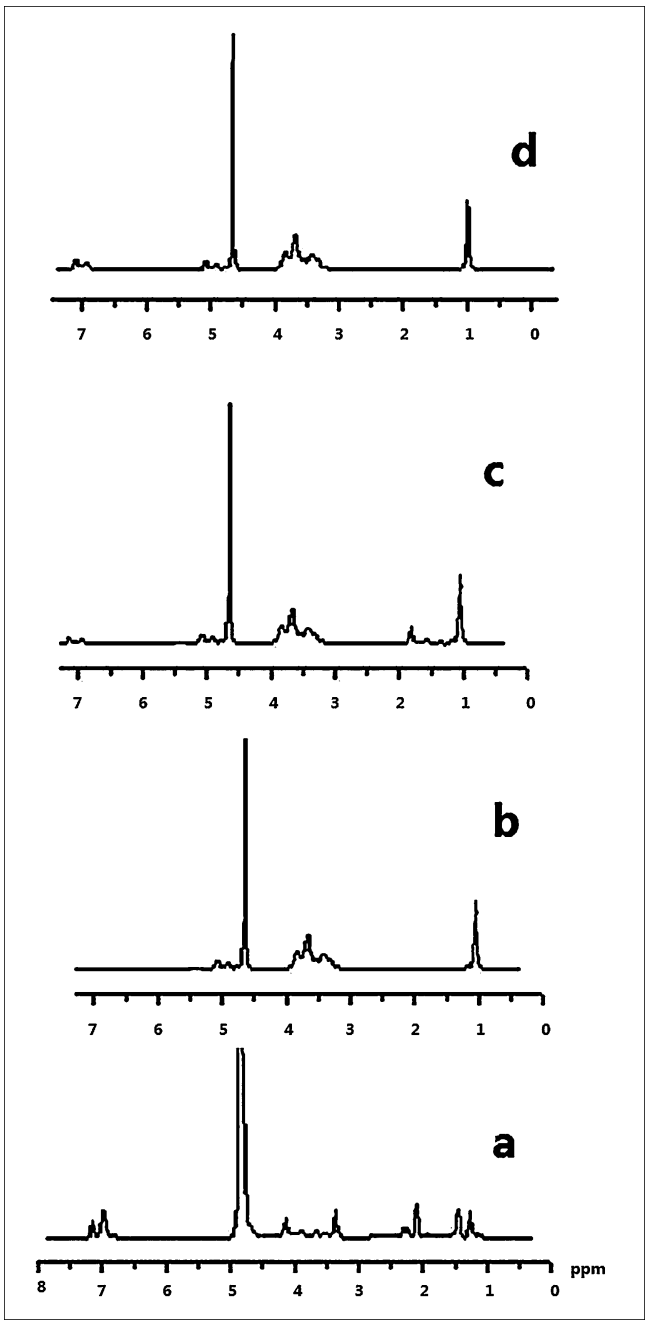

Fig. 8: ^{1}H NMR diagram. a: AT, b:HP-β-CD, c: AT/HP-β-CD inclusion complex (1:2), d: AT/HP-β-CD inclusion complex (1:6)

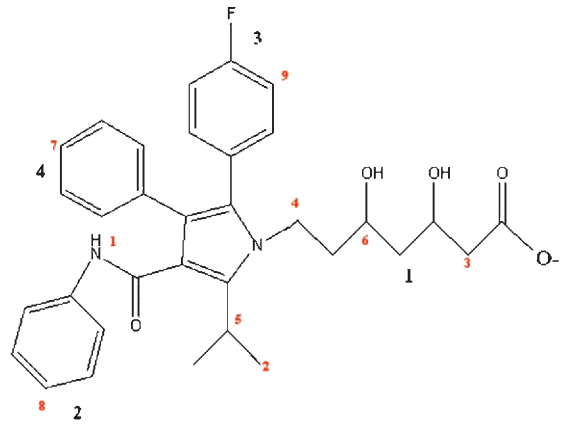

Fig. 9: Structure of AT

2.8. ODT tablets

The shape of the tablets of all formulations remained circular with no visible cracks. The average percentage weight variation of 20 tablets for each formulation remained within ± 3%. The drug content estimations showed values in the range of 99.12% to 102.17% which reflects good uniformity in drug content among different formulations. The hardness, friability and disintegration time of the two formulas are represented in Table 6.

All the formulations showed values within the prescribed limits for tests like hardness, friability and disintegration time which indicate that the prepared tablets are of standard quality. The good taste experienced from the inclusion complex showed a taste masking effect.

2.9. In vitro dissolution study

Fig. 10 shows the release rate profiles represented as percentage of drug dissolved verses time. Accordingly, the inclusion complex exhibits higher dissolution rates than the pure drug and Lipitor®. The inclusion complexes ODT (formula 2) released up to 99.05% of the drug in 5 min, and up to 101.65% after 15 min, whereas pure AT ODT exhibited a release of 34.48% after 5 min and less than 72.11% after 45 min. Lipitor® showed higher dissolution rates than the pure drug ODT, this could be attributed to solubilization effect of polysorbate 80 in the formulation (Lipitor 2006).

2.10. In vivo bioavailability study

Fig. 11 shows the mean plasma levels of the three tablets after oral administration to rats at an AT dose of 10 mg/kg. The pharmacokinetic parameters and the plasma concentration

Table 6: Hardness, friability and disintegration time of two formulas

Number	Mouth-feel	Friability percentage	Disintegration time	Hardness (kg/cm^3)
F1	A little bitter Taste, No gritty texture feeling, Ease of swallowing	0.67%	24 ± 3 s	4.5 ± 0.5 kg
F2	Good Taste, No gritty texture feeling, Ease of swallowing	0.61%	21 + 2 s	4.5 ± 0.5 kg

Note: F1: pure AT, F2: inclusion complex

Table 7: Pharmacokinetic parameters results (n = 12)

Parameter	F1	F2	Lipitor®
C_{max} (ng/ml)	526.87 ± 93.60	1977.91 ± 411.73	1392.67 ± 273.62
T_{max} (h)	1.0 ± 0.30	0.35 ± 0.17	0.5 ± 0.26
$AUC_{0-\infty}$(ng·h/ml)	2677.68 ± 324.29	11852.57 ± 1273.59	6358.66 ± 880.40
$T_{1/2}$(h)	4.31 ± 0.38	4.95 ± 0.29	4.75 ± 0.23
MRT(h)	6.06 ± 0.97	7.47 ± 1.13	6.97 ± 0.77
Relative bioavailability	42.11%(F1/Lipitor) 22.59%(F1/F2)	186.40%(F2/Lipitor) 442.64%(F2/F1)	

Note: F1: pure AT, F2: inclusion complex

time profiles are shown in Table 7, respectively. AT in Formula 2 showed rapid absorption (T_{max} = 0.35) as compared to Lipitor® (T_{max} = 0.5) and F1 (T_{max} = 1.0). C_{max} was also higher for F2 (1977.91 ± 411.73 ng/ml) above that of Lipitor® and F1 (1392.67 ± 273.62 and 526.87 ± 93.60 ng/ml respectively). Similarly F2 had the greatest Area Under the concentration time Curve (AUC) in the three formulas (Table 9). The difference between the groups, with regard to these parameters, was found to be significant at $p < 0.05$. Based on AUC the calculated relative bioavailability of F2: F1 and F2: Lipitor® was 442.64% and 186.40%, respectively.

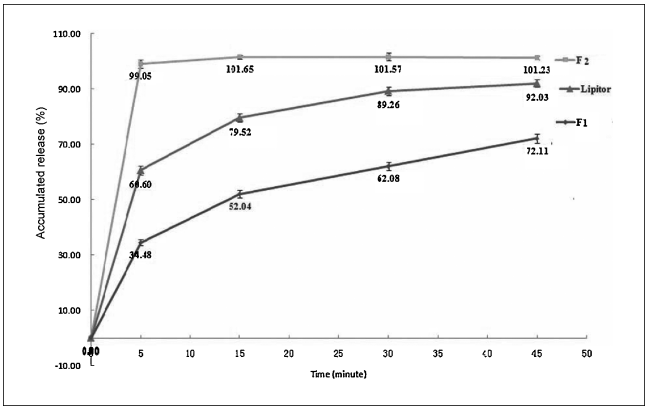

Fig. 10: Dissolution profiles of three tablets (F1: pure AT, F2: inclusion complex)

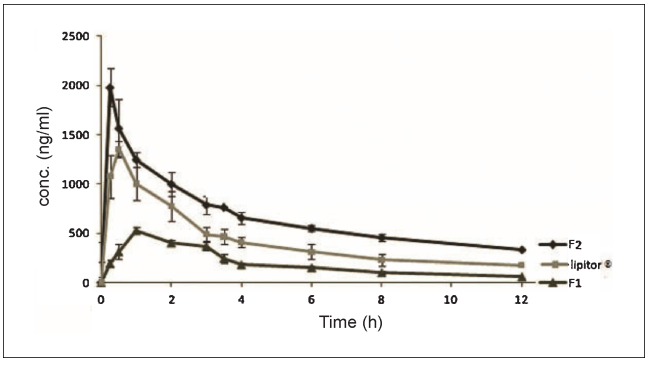

Fig. 11: Mean plasma concentration ± SD versus time curves for the three tablets (F1: pure AT, F2: inclusion complex)

From the results, it is obvious that there was an increase in the rate and extent of drug absorption from F2 (inclusion complex ODT) compared to F1 (pure AT ODT). Therefore, it is conceivable that inclusion complexation improves the solubility of the drug which in turn provides a much greater chance of absorption. However contrary to expectation, the enhancement in the extent of AT absorption from F2 was not significant (186.40%) compared to Lipitor®. This could be attributed to the experimental method used where the tablet was introduced directly into the stomach and hence suffered from the first pass metabolism effect. Ideally, a greater breakthrough is foreseen with administration of F2 (inclusion complex) in the conventional way of ODT evidently promising bioavailability enhancement to levels beyond that of the marketed tablet.

3. Discussion

In this study, ultrasound and rotary evaporating methods were applied to prepare the inclusion complex of AT with HP-β-CD. The phase solubility diagram was classified as A_N-type at all temperatures investigated, indicating the formation of the inclusion complex. DSC, ^{1}H NMR and FT-IR study indicated the presence of intermolecular hydrogen bonds between AT and HP-β-CD in the inclusion complex, and the result from PXRD study revealed that inclusion process keeps the amorphous form of AT.

In vitro dissolution studies indicated that the dissolution rates were remarkably increased in ODT of AT inclusion complex,

Table 8: Optimized ODT formulation

Ingredient	F1(mg)	F2(mg)
API	10	67
Mannitol	172	115
Low substituted Hydroxypropyl Cellulose	10	10
Cross carmellose sodium	10	10
Calcium carbonates	10	10
Aspartame	2	2
Magnesium stearate	1	1
Total	215	215

Note: API of F1 was 10 mg plain drug; API of F2 was 67 mg AT inclusion complex with HP-β-CD

compared to ODT of pure AT and Lipitor®. Moreover, the ODT of AT inclusion complex performed better than ODT of pure AT and Lipitor® in bioavailability in rats. This could be primarily attributed to the improved solubility and dissolution rate associated with inclusion complexing of AT and HP-β-CD. Based on this finding, the inclusion complex ODT of AT may be regarded a promising approach to enhance the bioavailability of AT upon confirmation in human volunteers.

4. Experimental

4.1. Materials

Amorphous atorvastatin calcium was kindly donated by Changzhou Pharmaceutical Co. Ltd. HP-β-CD was purchased from Xi'an Deli Biology & Chemical Industry Co., Ltd. Lipitor® was purchased from Nanjing drum tower hospital. Mannitol and aspartame was purchased from China Hui Xing biochemical reagent Co., Ltd. L-HPC (low substituted hydroxypropyl cellulose NF) was purchased from Shin-Etsu Chemical Co., Ltd. Japan. AC-DI-SOL® (croscarmellose sodium) purchased from FMC Corporation USA. Calcium carbonate and magnesium stearate were purchased from Nanjing Chemical Reagent Factory China. All the reagents were of analytical grade.

4.2. Methods

4.2.1. Molecular-modeling studies

Docking simulation was performed using Dock Ligands (CDOCKER) program in Discovery Studio (DS) 2.1 (Accelrys, Inc., CA). Prior to docking the three dimensional structure of atorvastatin was retrieved from the drug bank website (http://drugbank.wishartlab.com/) with accession number DB01076, while the three dimensional structure of HP-β-CD was built up using ACD/Chem sketch freeware version 10 (build 13206, 31 AUG 2006). Before running the Dock Ligands (CDOCKER) program, energy minimization of both molecules was conducted using CharmM minimization program in DS 2.1. The smart minimizer algorithm was employed to perform the minimization process. The resulting typed MMFF force molecules were used as receptor and ligand for HP-β-CD and atorvastatin, respectively. From the conformations of 10 top hits, only the least energy pose was chosen to calculate the complex energy and the interaction energy. This was facilitated by programs for calculating energy and interaction energy in the simulation directory of DS 2.1.

4.2.2. Phase-solubility studies

The phase-solubility technique was utilized for evaluation of the affinity between HP-β-CD and AT in water. Phase-solubility studies were performed according to the method reported by Higuchi and Connors (1965). Briefly excess amounts of drug (approx. 300 mg AT) were added to 100 ml vials containing 50 ml aqueous solutions of increasing concentrations of HP-β-CD (0–100 mM/ml) and shaken at 25 °C, 35 °C and 45 °C for 24 h to reach equilibrium. Sampling was done subsequently by withdrawing aliquots using a syringe; the samples were immediately filtered through a 0.45 μm micro-porous membrane and appropriately diluted. HPLC analysis was then performed on a LC-2010, Shimadzu, Japan, with the mobile phase comprising of a mixture of menthol and 0.03 mol/L sodium phosphate in water (70:30 v/v). The column (C_{18}, 150 mm × 4.6 mm i.d, 5 μm) was maintained at 25 °C, injection volume was 20 μL at a flow rate of 1.0 ml/min and the effluent detected at 241 nm. The phase solubility profile was drawn according to concentration of HP-β-CD and AT.

4.2.3. Preparation of the inclusion complex and physical mixture

The preparation of solid complexes was performed by three techniques (grinding method, ultrasound method and stirring method). Various ratios of AT and HP-β-CD were dispersed into ethanol solution before using the three techniques in parallel as follows, grinding for 2 h, sonicating for 30 min and stirring for 12 h at room temperature. The suspensions were rotary evaporated to remove the alcohol. The resultant complex was dissolved in 10 ml distilled water and filtered through a 0.22 μm microporous membrane. The filtrate was frozen and then lyophilized.
Pure AT and the prepared inclusion complexes were added to 10 ml vials containing distilled water (5 ml) and shaken for 24 h to reach equilibrium. Samples were filtered through a 0.45 μm micro-porous membrane and determined by HPLC as in item 4.2.2. The solubility and entrapment efficient of the inclusion complex were calculated according to drug content.
A physical mixture consisting of HP-β-CD and AT in 1:6 ratio as lyophilized complex was also prepared by mixing HP-β-CD and AT in a beaker and stirring for 3 min to obtain a homogeneous blend.

4.2.4. Characterization

4.2.4.1. Differential scanning calorimetry (DSC). The samples were analyzed by a DSC204 (NETZSCH, Germany) at a scanning rate of 10 °C/min. Accurately weighed samples (2.4 mg) were placed in sealed aluminum pans and scanned over a temperature range of 30 °C to 350 °C at 10 °C/min. An empty aluminum pan was used as reference.

4.2.4.2. X-ray diffraction studies (XRD). Powder X-ray diffraction diagrams were obtained with a Bruker D8 Advance powder diffraction meter (BRUKER-AXS, Germany) with Cu K α radiation in the range of 5–60° (2θ) at 40 kV and 30 mA. Step scan mode was adopted with a step size of 0.02° at a rate of 3°/min. The process parameters were set to step size of 0.05° (2θ), scan step time of 0.5 s.

4.2.4.3. Fourier transforms infrared spectroscopy (FT-IR). FT-IR spectra of samples were recorded with a BRUKER-MPA spectrometer (BRUKER, Germany) by KBr disc method in the wave range of 400–5000 cm^{-1}.

4.2.4.4. ^{1}H-Nucleaur Magnetic Resonance (H NMR). ^{1}H NMR spectra of the inclusion complex were obtained with an AVANCE II spectrometer (BRUKER, Germany) at 400 MHz using 0.5 mL d6-DMSO as solvent, relaxation delay 2.0 s with a mixing time of 2.00 min.

4.2.5. ODT tablets preparation

After several preliminary trails, the ODT formulations; F1 (pure AT) and F2 (inclusion complex) were optimized according to hardness and disintegration times (Table 8). Circular tablets with 2 mm thickness were produced by a direct compression method using an 8 mm flat facetted punch (TDP, shanghai, China). The hardness and friability of ODT was determined using a YD-20 intelligent tablet hardness tester (Tianjin technical company, China). Disintegration time was estimated *in vitro* using USP method for disintegration testing recommended by FDA (FDA 2008).

4.2.6. In vitro dissolution studies

Dissolution studies were carried out by USP Apparatus 2 (paddle) method (D-800LS, Tianjin, China) at 50 rpm/min and 37 ± 0.5 °C. Three tablets each for F1, F2 and Lipitor®, were added into beakers containing 900 ml of the distilled water equilibrated to 37 ± 0.5 °C. Samples (5 ml) were withdrawn at 5, 15, 30, 45 min intervals and filtered through a 0.8 μm micro-porous membrane, replenishing with fresh medium. The filtrate was diluted with methanol and assayed by HPLC system.

4.2.7. In vivo bioavailability studies

4.2.7.1. Animals and blood samples. Up to 36 Sprague-Dawley used (210 ± 10 g body weight) and treated according to the regulations for animal care of China Pharmaceutical University. The rats were allowed free access to food and water but were fasted for 12 h before drug administration. 36 rats were randomly divided into three groups of 6 males and 6 females per group. Powders (contains AT 25 mg/kg) of F1, F2 and Lipitor® separately suspended in 1.5 ml water were administrated to the rats as per group. The rats were anesthetized by ethyl ether. Blood (0.5 ml) was collected using an orbital sinus venipuncture by capillary tubes from the rats at set time points as 0 (before administration), 15, 30, 60, 120, 180, 210, 240, 270, 480 and 720 min after the administration.
The blood samples were drawn into pre-labeled heparin containing tubes and plasma separated within 30 min by centrifugation at 4000 rpm for 10 min at room temperature. The plasma was stored at –20 °C in labeled polypropylene tubes until HPLC analysis.
Frozen plasma samples were thawed at ambient temperature. In a 5 ml polypropylene centrifuge tube, a 150 μL aliquot of plasma with 150 μL internal standard solution (diclofenac sodium solution, 1 μg/mL) and 3 ml of acetic ether were blended by vortexing for 5 min and then centrifuged at 4000 rpm for 10 min. The organic layer was transferred to a clean, dry 2 ml polypropylene centrifuge tube and the sample evaporated to dryness under a stream of nitrogen at 40 °C. The dry residue was reconstituted with 150 μL mobile phase. A 20 μL aliquot of the sample was injected onto the column for HPLC analysis, mobile phase as a mixture of methyl cyanides and 0.03 mol/L ammonium acetate solution (50:50 v/v). The column (C_{18}, 150 mm × 4.6 mm i.d, 5 μm, Shimadzu, Japan) was maintained at 25 °C with a flow rate of 1.0 mL/min and effluent detected at 241 nm.

4.2.7.2. Pharmacokinetic analysis. Pharmacokinetic parameters were calculated using the software Thermo kinetica version 4.4.1. The differences between the groups in terms of C_{max} and AUC were tested using ANOVA

followed by post hoc tests using S-N-K method. And the differences between groups regarding T_{max} were examined by Kruskal Wallis test.

Acknowledgements: This work was supported by The National Natural Science Foundation of China (No. 30901867) and The National Science and Technology of China for new drugs development with No. 2009ZX09310-004.

References

Ben Zirar S, Astie A, Muchow M, Gibaud S (2008) Comparison of nanosuspensions and hydroxypropyl-β-cyclodextrin complex of melarsoprol: Pharmacokinetics and tissue distribution in mice. Eur J Pharm Biopharm 70: 649–656.

Cabral Marques HM, Hadgraft J, Kellaway IW, Pugh WJ (1990) Studies of cyclodextrin inclusion complexes. Part 2. Molecular modeling and proton NMR evidence for the salbutamol-β-cyclodextrin complex. Int J Pharm 63: 267–274.

Crupi V, Ficarra R, Guardo M, Majolino D, Stancanelli R, Venuti V (2007) UV-vis and FTIR-ATR spectroscopic techniques to study the inclusion complexes of genistein withβ-cyclodextrins. J Pharm Biomed Anal 44: 110–117.

FDA (2008) Guidance for Industry Orally Disintegrating Tablet.

Foody JM, Joyce AT, Rudolph AE, Liu LZ, Benner JS (2008) Cardiovascular outcomes among patients newly initiating atorvastatin or simvastatin therapy: a large database analysis of managed care plans in the United States. Clin Therap 30: 195–205.

Frömming KH, Szejtli J (1994) Cyclodextrin in Pharmacy; Kluwer Academic Publishers. Dordrecht.

Gould S, Scott RC (2005) 2-Hydroxypropyl beta cyclodextrin: a toxicological review. Food Chem Toxicol 43: 1451–1459.

Higuchi T, Connors KA (1965) Phase-solubility techniques. Adv Anal Chem Instr 4: 117–122.

Kappelle PJ, Dallinga-Thie GM, Dullaart RP (2010) Atorvastatin treatment lowers fasting remnant-like particle cholesterol and LDL subfraction cholesterol without affecting LDL size in type 2 diabetes mellitus: Relevance for non-HDL cholesterol and apolipoprotein B guideline targets. Biochim Biophys Acta 1801: 89–94.

Khedr A (2007) Stability-indicating high-performance liquid chromatographic assay of atorvastatin with fluorescence detection. J AOAC Int 90: 1547–1553.

Kim MS, Jin SJ, Kim JS, Song HS, Neubert RH, Hwang SJ (2008) Preparation, characterization and *in vivo* evaluation of amorphous atorvastatin calcium nanoparticles using supercritical antisolvent (SAS) process. Eur J Pharm Biopharm 69: 454–465.

Lipitor (2006) http://www.fda.gov/ohrms/DOCKETS/ac/06/briefing/2006-4254b_16_02_KP%20Atorvastatin%20Label%20FDA%208-7-06.pdf.

Loftsson T, Brewster ME (1996) Pharmaceutical applications of cyclodextrins. 1: Drug solubilization and stabilization. J Pharm Sci 85: 1017–1025.

Yaksh TL, Janq JD, Nishiuchi Y, Braun KP, Ro SG, Goodman M (1991). The utility of 2-hydroxypropyl beta cyclodextrin as a vehicle for the intracerebral and intrathecal administration of Drugs. Life Sci 48: 623–634.

Yang J, Wiley CJ, Godwin DA, Felton LA (2008) Influence of hydroxypropyl-β-cyclodextrin on transdermal penetration and photostability of avobenzone. Eur J Pharm Biopharm 69: 605–612.

Simons J (2003) The $10 Billion Pill Hold the fries, please. Lipitor, the cholesterol-lowering drug, has become the best selling pharmaceutical in history. Here's how Pfizer did it, Fortune magazine, January 20.